Elmesallamy
Egyptian Journal of Neurosurgery (2024) 39:24
https://doi.org/10.1186/s41984-024-00279-4

Egyptian Journal of Neurosurgery

RESEARCH Open Access

Gross pathology of brain mass lesions by intraoperative ultrasonography: a comparative study

Wael Abd Elrahman Ali Elmesallamy[1*]

Abstract

Background The purpose of this study was to evaluate the ability of intraoperative ultrasound (IOUS) to differentiate the gross pathological features of brain mass lesions in comparison with preoperative imaging and confirmable histopathological results.

Results A total of 365 patients were operated on for brain mass lesions removal from May 2017 to May 2022 under the guidance of intraoperative ultrasound with transducers 2.5–8 megahertz (MHZ). Ultrasound gross pathological findings were compared to the preoperative imaging and the confirmable histopathological results. Intraoperative ultrasound defined either internal or external gross pathological features of all brain mass lesions. The IOUS showed spontaneous enhancements of the brain abscess walls, which were equivalent to contrasted CT and MRI. Significantly large diameters were noted in the IOUS measurement of abscesses in comparison with CT and MRI ($P=0.001$). The walls of the brain abscesses were significantly well defined in IOUS imaging in comparison with CT ($P=0.001$) and equivalent to MRI. IOUS showed equivalent significance to CT and MRI in characterizing intra-parenchymal hematomas. Significantly large diameters were noted in the IOUS measurement of hematomas in comparison with CT and MRI ($P=0.001$). IOUS showed significant definition of brain tumors in comparison with CT and MRI regarding tumor edge definition, tumor contours, necrosis, and cystic components (cystic definition, cystic multiplicity, cystic trabeculations, and cystic wall thickness) ($P=0.001$). IOUS was equivalent to CT and MRI regarding intratumoral hematomas and brain edema. IOUS was equivalent to CT regarding calcification detection. The significant criteria for high-grade brain tumors versus low grade by IOUS were: $P=0.001$ (necrosis, brain edema, rare calcifications, presence of cystic components, thick cystic walls, large diameter, hypo-echogenicity, and heterogeneity); $P=0.002$ (cystic trabeculations); $P=0.005$ (multiple cysts); and $P=0.03$ (irregular contour). IOUS can characterize brain tumors and suspect specific and significant criteria for many types with great overlap.

Conclusions Intraoperative ultrasound has the ability to differentiate the gross pathological features of brain mass lesions in comparison with preoperative imaging and confirmable histopathological results.

Keywords Intraoperative ultrasound, Brain mass lesions, Pathological criteria, Brain abscesses, Brain tumors, Malignant criteria

Background

Intraoperative ultrasound (IOUS) is noninvasive, easily movable, fast, and cheaper than intraoperative MRI. Regarding brain tumors identification and anatomical relations, it provides real-time and high-quality images, facilitating control of the operative process [1, 2]. Ultrasound has been used intraoperatively for decades to differentiate

*Correspondence:
Wael Abd Elrahman Ali Elmesallamy
waelmesallamy@gmail.com
[1] Neurosurgery Department, Faculty of Medicine, Zagazig University, Zagazig, Egypt

solid, cystic, necrotic, and fleshy tissues according to their different acoustic impedances and reflection coefficients [3]. Every type of brain tumors has been well imaged by IOUS. Low-grade gliomas are better defined with ultrasound than computed tomography. Abscesses and hematomas are well imaged by IOUS [4]. The intraoperative ultrasound had significant agreement with histopathology compared to MRI T1 regarding low-grade gliomas [5]. The power of ultrasound signal reflection is determined by tissue components and can indicate the pathology of the lesions. Echogenicity is determined in relation to adjacent brain parenchyma. Hypo-echoic tissues mean elevated water content or elevated cellularity, whereas hyper-echoic tissues mean high stromal components or rich capillaries [6]. The ultrasound machine depends on the change in acoustic impendence of the tissues across the wave pathway, while the MRI machine depends on the relative concentration of H nuclei in the different tissues [7].

The purpose of the study was to evaluate the reliability of intraoperative ultrasound for detection of the gross pathological criteria of the brain mass lesions in comparison with preoperative CT, preoperative MRI, and confirmable histopathological results.

Methods

This comparative study was carried out at Zagazig University Hospitals from May 2017 to May 2022 and approved by the institutional review board (Zu-IRB #9654). The study population consisted of 365 patients.

Inclusion criteria were non-traumatic brain mass lesions (tumors, abscesses, and intra-parenchymal hematomas), which indicated for surgical removal. Exclusion criteria were; recurrent brain masses; irradiated brain masses; and traumatic lesions.

Procedures

All patients were operated on under general anesthesia, and consents for the procedure were obtained according to the local research ethics committee in our neurosurgery department. Intraoperative 2D (dimensions) ultrasound was used during surgeries for all patients; IBE-2500D digital ultrasound with endo-cavitary transducer (5, 6.5, and 8 MHZ) of foot diameters 18×8 mm and electronic convex transducer (2.5, 3.5, and 5 MHZ) of foot diameters 50×12 mm. The deep lesions near the midline of the brain are best delineated by low frequencies (3.5, 5 MHZ), while superficial lesions are best delineated by high frequencies (6.5, 8 MHZ); as is known, the reverse relationship exists between frequency and both depth and resolution clearance (low-frequency waves represent low image resolution but can penetrate deeper because of a low degree of wave attenuation). The probe is inside a sterile surgical sheath with acoustic gel trapped in front of it. The real-time and B-modes were used during the surgical procedure. For best spatial resolution of the brain and the mass lesions, multiple factors must be adjusted during ultrasound imaging: head position (permits saline to stay in the surgical cavity), probe (proper size according to the working area, proper frequency according to the lesion depth), scanner parameters (brightens, depth, gain, focus), and surgical field (air and blood elimination, gel and saline connection, avoid the presence of surgical instruments, and any foreign materials). The ultrasound was used after skull bone removal for delineation of the mass, both internal or external characters in comparison with preoperative images (CT and MRI T1 of 1.5 Tesla) and postoperatively confirmed pathology. The mass lesions were evaluated for external and internal characteristics in B-mode ultrasound by the author, who has experience in ultrasound use during brain surgeries since 2007. The CT and MRI were reported by radiology consultants.

Measurement parameters

- Brain lesion wall definition by IOUS was defined according to Mair et al. [8] grading system, which graded visibility of brain mass lesions and borders by IOUS into 4 grades: grade 0 (not visible), grade 1 (poor visibility and borders), grade 2 (good visibility and poor borders), and grade 3 (good visibility and clear border). During our work, all brain mass lesions were defined as well defined (Mair grade 3) and ill defined (Mair grade 2), as we did not face any grade 1 or 0 according to Mair grading.
- Brain tumors grading criteria were done according to the WHO (World Health Organization) grading and classification system [9]. Gross criteria evaluated in the three imaging modalities included mass wall, contour, shape, size, color in relation to brain tissues, homogeneity, enhancement, surrounding edema, and internal components including necrosis, hematoma, calcification, and cystic structures.
- Intra-parenchymal hematomas aging were classified as acute 2 days, sub-acute 3–14 days, and chronic > 14 days.

Statistical analysis

All data were collected, tabulated, and statistically analyzed using IBM Corp. Released 2015. IBM SPSS Statistics for Windows, version 23.0 Armonk, NY: IBM Corp. Quantitative data were expressed as the median (range), and qualitative data were expressed as numbers and percentages. The Mann–Whitney test compared two variables that were non-normally distributed. The Wilcoxon sign rank test was used to compare pairs of non-normally distributed variables. The McNemar test was used to compare pairs of categorical value variables. Cochran's Q test was

used to determine if there are differences in a dichotomous dependent variable between three or more related groups. The Friedman test was used to test for differences between groups when the dependent variable being measured has deviations from normality. Percentages of categorical variables were compared using the Chi-square test or Fisher exact test when appropriate. All tests were two-sided. A P value < 0.05 was considered statistically significant; a P value ≥ 0.05 was considered statistically insignificant.

Results

A total of 365 patients were subjected to the surgical removal of brain mass lesions. Ages ranged from 3 months to 72 years old with a mean of 49 years; males were 235, 64.4% patients, and females were 130 patients with a ratio of 1.8:1.263, 72% of the patients were operated for brain tumors, 61 patients were operated for intra-parenchymal hematomas, and 41 patients were operated for brain abscesses. The supra-tentorial location of the mass lesions was found in 274 patients (5% of the patients). Table 1

Table 1 Patients and brain mass lesions data

Parameters	Number of patients	%
Age		
Range (3 months:72 years)		
Mean (49 years)		
Sex		
Males	235	64.4
Females	130	35.6
Pathology		
Tumors	263	72
Hematomas	61	17
Abscesses	41	11
Site to tentorium cerebelli		
Supratentorial	274	75
Infratentorial	91	25

Brain abscesses

The number of patients operated on for brain abscesses was 41, with 53 abscesses (32 patients with a single abscess, six patients with two abscesses, and three patients with three abscesses). The gross pathological features of brain abscesses by IOUS, preoperative CT with contrast, and preoperative MRI with contrast; the multiplicity (single or multiple), shape (round or oval), and brain edema were detected by all of the three imaging modalities without significant differences. The IOUS showed spontaneous enhancements of the brain abscess walls, which were equivalent to contrasted CT and MRI. In all cases, the contents of the brain abscesses were hypo-echogenic in IOUS imaging, hypo-dense in CT imaging, and hypo-intense in MRI T1 imaging in relation to brain tissues. Significantly large diameters were noted in the IOUS measurement in comparison with CT and MRI ($P = 0.001$). The walls of the brain abscesses were significantly well defined in IOUS imaging in comparison with CT ($P = 0.001$) and equivalent to MRI. Table 2

Table 2 Brain abscesses gross pathology (41 patients with 53 abscesses)

Parameters	Preoperative CT	Preoperative MRI T1	IOUS	*P*
Number				
Single	32 (78%)	32 (78%)	32 (78%)	1
Multiple	9 (22%)	9 (22%)	9 (22%)	
Shape				
Round	30 (56.6%)	30 (56.6%)	30 (56.6%)	1
Oval	23 (43.4%)	23 (43.4%)	23 (43.4%)	
Diameter in centimeter				
Median (range)	2.9 (0.05–4)	3.4 (0.7–4.3)	3.6 (0.9–5)	0.001*
Wall				
Well defined	40 (75.5%)	53 (100%)	53(100%)	0.001*
Ill defined	13 (24.5%)	0	0	
Contrast enhancement	50 (94%)	53(100%)	Spontaneous 53 (100%)	0.15
Content	53 (100%)	53 (100%)	53 (100%)	1
	Hypo-dense	Hypo-intense	Hypo-echoic	
Edema	53 (100%)	53 (100%)	53 (100%)	1

*$P < 0.05$ significant

IOUS (intraoperative ultrasound), CT (computed tomography), MRI (magnetic resonance imaging)

Demonstration of brain abscesses by the three imaging modalities (IOUS, MRI, and CT) and operative specimens of five different cases (a, b, c, d, and e) presented in Fig. 1.

Hematomas

The number of patients operated on for intra-parenchymal hematomas was 61. The gross pathological features of brain hematomas by IOUS, preoperative CT, and

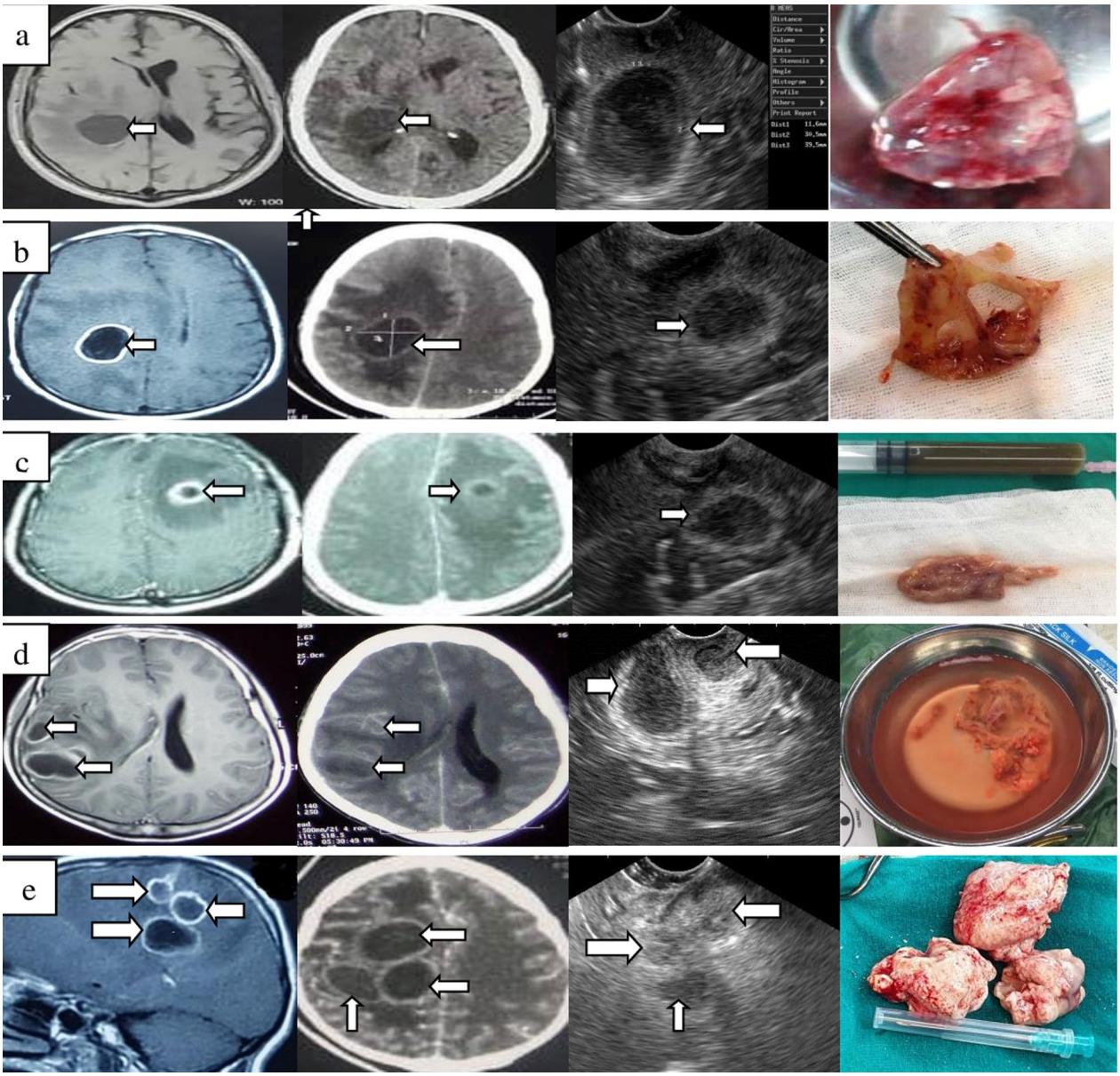

Fig. 1 Brain abscesses imaging by MRI with contrast, CT with contrast and IOUS and operative specimens. White arrows point to the wall of the abscesses. Case **a**: Single brain abscess; enhanced wall, hypo-intense content and surrounded by hypo-intense edema in MRIT1 with contrast. Enhanced wall, hypo-dense content, and surrounded by hypo-dense edema in CT with contrast. Spontaneous enhanced wall, heterogeneous hypo-echoic content and surrounded by hyper-echoic edema in IOUS B-Mod. Thick and smooth wall of the operative specimen. Case **b**, **c** differ from (**a**) in the intraoperative specimen as the wall is thin, smooth, and friable. Case **d**: Two brain abscesses with same characters as (**b**, **c**) but less CT delineation of both abscesses especially the anterior one with time lapse less than 48 h between the three types of imaging modalities. Case **e**: Three abscesses with similar characters as (**a**) but rough specimen surface. The noted low resolution of ultrasound image can be explained by the use of low frequency 3 MHZ to reach far depth to delineate all of the lesions, but during resection we used step wise high frequencies 5–8 MHZ for superficial abscesses for better resolution, and then, the deepest one was also better delineated through the resection cavity by high frequencies

Table 3 Brain hematomas gross pathology (61 patients)

Parameters	Preoperative CT	Preoperative MRI T1	IOUS	*P*
Shape				
Round	7 (11.5%)	7 (11.5%)	7 (11.5%)	1
Oval	22 (36%)	22 (36%)	22 (36%)	
Irregular	32 (52.5%)	32 (52.5%)	32 (52.5%)	
Diameter in centimeter				
Median (range)	5 (2.5–8)	5.5 (2.7–8.1)	5.7 (2.9–8.8)	0.001*
Well-defined edge	61 (100%)	61 (100%)	61 (100%)	1
Edema	20 (32.8%)	20 (32.8%)	20 (32.8%)	1
Color				
Acute ≤ 2 days	Hyper-dense	Hypo-intense T1, T2	Hyper-echoic	
Early sub-acute 3–7 days	Mixed	Hyper-intense T1	Mixed	
Late sub-acute 8- 60 days	Iso or hypo-dense	Hyper-intenseT1, T2	Hypo-echoic	
Chronic > 60 days	Hypo-dense	Hypo-intenseT1, T2		

*$p < 0.05$ significant

IOUS (intraoperative ultrasound), CT (computed tomography), MRI (magnetic resonance imaging)

preoperative MRI T1; the shape (round, oval, or irregular), edge definition, and brain edema were detected by all of the three imaging modalities without significant differences. Color changes with time were defined in the imaging modalities. Significantly large diameters were noted in the IOUS measurement in comparison with CT and MRI (PP = 0.001). Table 3

Demonstration of intra-parenchymal brain hematomas by the three imaging modalities (IOUS, MRI, and CT) in three different cases (a, b, and c) presented in Fig. 2.

Tumors

IOUS showed significant abilities in characterizing brain tumors in 263 patients.

IOUS versus CT and MRI

Comparing preoperative (CT, MRI T1) and IOUS tumors characteristics;

- IOUS showed significant definition of brain tumors in comparison with CT regarding tumor edges definition, tumor contours, necrosis, cystic components (cystic definition, cystic multiplicity, cystic trabeculations, and cystic wall thickness), hyper-gray scale, and heterogeneity ($P = 0.001$). IOUS was equivalent to CT regarding calcification, intra-tumoral hematomas, and brain edema.
- IOUS showed significant definition of brain tumors in comparison with MRI T1 regarding tumor edges, tumor contours, necrosis, calcification, cystic components (cystic definition, cystic multiplicity, cystic trabeculations, and cysts with thin walls), and hyper-gray scale ($P = 0.001$). IOUS was of significance in the definition of thick walls of cysts and heterogeneity in comparison with MRI ($P = 0.016$ and 0.03, respectively). IOUS was equivalent to MRI T1 regarding intra-tumoral hematomas and brain edema.
- Preoperative MRI T1 showed significant definition of brain tumors in comparison with CT regarding tumor edge delineation, tumor contour definition, necrosis, cystic components, and heterogeneity ($P = 0.001$). MRI T1 was equivalent to CT regarding intra-tumoral hematomas and brain edema. However, CT significantly defined calcification in comparison with MRI T1 ($P = 0.001$). Table 4

With these findings, we can find that IOUS gains the benefits of CT in defining calcification and MRI in defining other important pathological features in real-time fashion during surgeries.

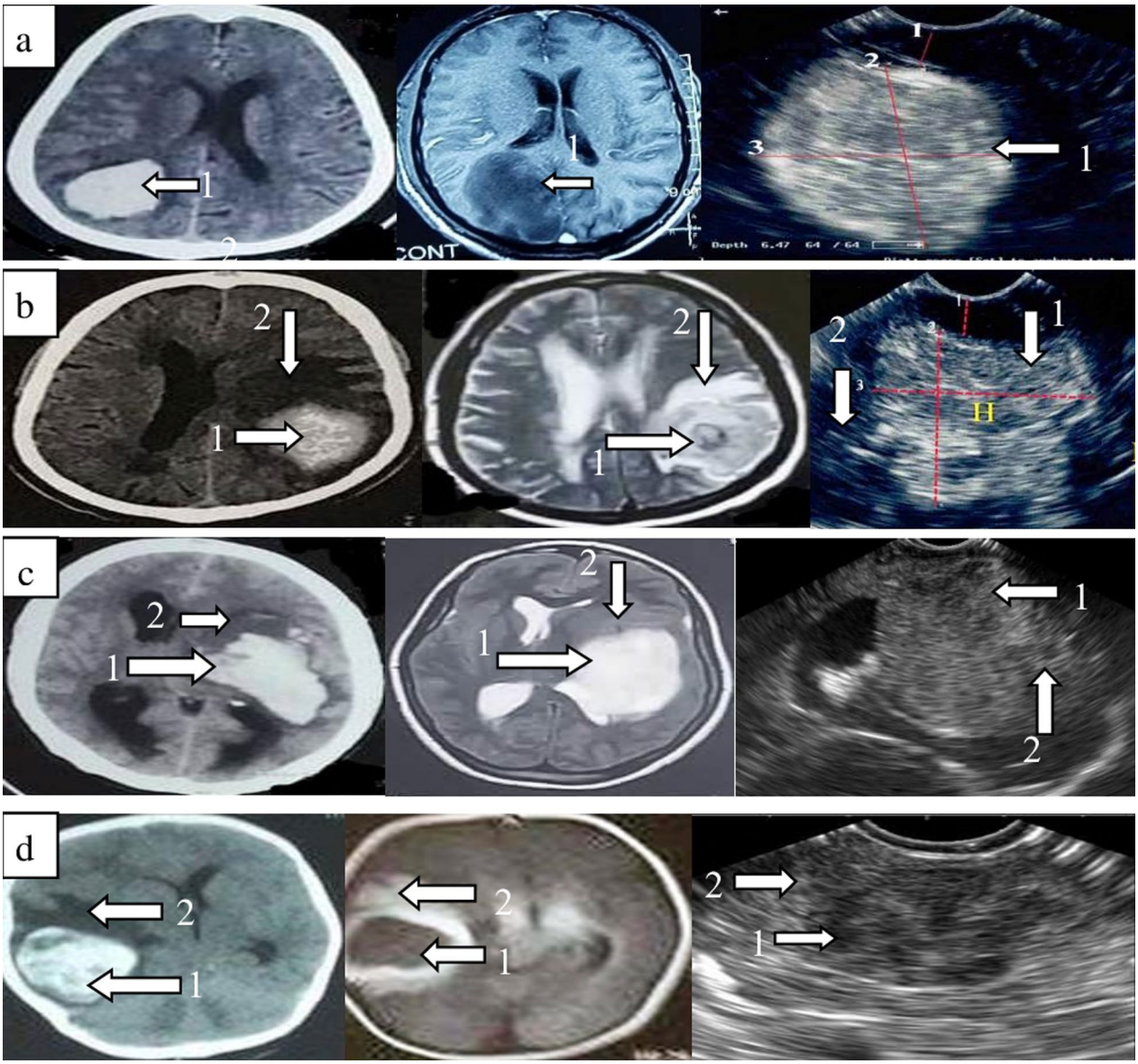

Fig. 2 Imaging of intracerebral hematomas by CT, MRI, and IOUS. Arrows 1 refer to the hematoma and arrows 2 refer to brain edema. Case **a**: Acute intracerebral hematoma; homogenous hyper-dense in CT on day 1, homogenous hypo-intense in MRI T1 on day 1 and heterogeneous mostly hyper-echogenic in IOUS on day 2. Case **b**: Early sub-acute intracerebral hematoma; hyper-dense mostly homogenous in CT on day 5, heterogeneous hypo-intense in MRI T1 with contrast on day 6 and heterogeneous mostly hyper-echogenic in IOUS on day 7. Case **c**: Intracerebral hematoma; hyper-dense mostly homogenous in CT on day 5, homogenous hyper-intense in MRI on day 15 (late sub-acute) and homogeneous iso-echogenic in IOUS on day 15. Case **d**: Intracerebral hematoma; heterogeneous mixed densities in CT on day 10, homogenous hypo-intense in MRI on day 60 and heterogeneous hypo-echogenic in IOUS on day 60

IOUS and WHO (World Health Organisation) grading [9]

Trying to find the significant criteria for high-grade brain tumors by IOUS: $P=0.001$ (necrosis, brain edema, rare calcifications, presence of cystic components, thick cystic walls, large diameter, hypo-echogenicity, and heterogeneity), $P=0.002$ (cystic trabeculations), $P=0.005$ (multiple cysts), and $P=0.03$ (irregular contour). Table 5

Table 4 Brain tumors gross pathology according to CT, MRI, and IOUS investigation

	CT		MRI		IOUS		*P*		
	n	%	n	%	n	%	CT versus IOUS	MRI versus IOUS	CT versus MRI
Well-defined edge	120	45.6	198	75.3	240	91.3	0.001*	0.001*	0.001*
Regular contour	84	31.9	138	52.5	154	58.6	0.001*	0.001*	0.001*
Necrosis	61	23.2	125	47.5	146	55.5	0.001*	0.001*	0.001*
Hematoma	11	4.2	11	4.2	11	4.2	1	1	1
Calcification	38	14.4	12	4.6	37	14.1	1	0.001*	0.001*
Edema	225	85.6	225	85.6	225	85.6	1	1	1
Cysts	106	40.3	129	49.0	168	63.9	0.001*	0.001*	0.001*
Single	40	15.2	53	20.2	77	29.3	0.001*	0.001*	0.001*
Multiple	66	25.1	76	28.9	91	34.6	0.001*	0.001*	0.001*
Trabeculation	10	3.8	20	7.6	42	16.0	0.001*	0.001*	0.001*
Thin wall	40	15.2	52	19.8	85	32.3	0.001*	0.001*	0.001*
Thick wall	60	25.1	77	29.3	84	31.9	0.001*	0.016*	0.04*
Diameter in centimeter									
Median (range)	4.8(1.5–10)		5(1.7–10.1)		4.9(1.9–10.8)		0.06	0.065	0.55
Color (main gray scale)									
Hypo	226	85.9	235	89.4	86	32.7	0.001*	0.001*	0.022*
Hyper	37	14.1	28	10.6	177	67.3			
Homogeneity									
Homogeneous	95	36.1	61	23.2	55	20.9	0.001*	0.03*	0.001*
Heterogeneous	168	63.9	197	76.8	208	79.1			

*$P < 0.05$ significant

IOUS (intraoperative ultrasound), CT (computed tomography), MRI (magnetic resonance imaging)

IOUS and different tumor types

It is difficult to organize specific criteria for each tumor type (according to the WHO classification of brain tumors) by gross pathological features of any imaging modalities, as brain tumors include a lot of types beside that, the microscopic examination and other investigations like proliferative factors, tumor markers may be needed to reach the real tumor type. IOUS can characterize brain tumors and suspect specific and significant criteria for many types, with overlaps.

High-grade criteria by IOUS were applied to differentiate low-grade gliomas from high-grade gliomas and also to other tumor types.

- Gliomas showed significant ($P=0.001$) for; necrosis (HG), edema (HG), cystic components (HG), thick cystic walls (HG), heterogeneous echogenicity (HG), calcification (LG), and hyper-echogenicity (LG). Multiple cysts (HG) $P=0.007$; cystic trabeculations (HG) $P=0.004$; and a thin cystic wall (LG) $P=0.009$. Figures 3, 4, and 5
- By comparing gliomas, metastases, meningiomas, and other brain tumors (medulloblastoma, choroid plexus papilloma, and intraventricular epidermoid).
- Regular contour was found to be significantly associated ($P=0.001$) with meningiomas (90% of meningiomas presented by regular contour, followed by other tumors 88%, metastasis 74%, and gliomas 43%).
- Necrosis was significantly associated ($P=0.001$) with metastases (77% of metastases presented by necrosis, followed by gliomas 58%, other tumor types 43%, and meningiomas 20%).
- Calcifications were found significantly ($P=0.004$) in meningiomas (45% of meningiomas had calcifications, gliomas 15%, other tumors 12%, and metastases 0%).
- Edema was found significantly ($P=0.001$) with metastases at 100%, gliomas at 94%, other tumors at 83%, and meningiomas at 50%.
- Hyperechogenicity was found significantly ($P=0,001$) in meningiomas (100%), other tumors (76%), gliomas (67%), and metastases (44%). Notice that metastases are the most common hypo-echoic mass lesion but may be hyper-echoic.

Table 5 Brain tumors grading; high grade (HG) versus low grade (LG) according to CT, MRI T1, and IOUS investigation

	CT				*P*	MRI				*P*	IOUS				*P*
	High grade n.202		Low grade n.61		CT	High grade n.202		Low grade n.61		MRI	High grade n.202		Low grade n.61		IOUS
	n	%	n	%		n	%	n	%		n	%	n	%	
Well-defined edge	83	41.1	37	60.7	0.007*	147	72.8	51	83.6	0.086	182	90.1	58	95.1	0.31
Regular contour	55	27.2	29	47.5	0.003*	97	48.0	41	67.2	0.009*	111	55.0	43	70.5	0.03*
Necrosis	61	30.2	0	.0	0.001*	121	59.9	4	6.6	0.001*	141	69.8	5	8.2	0.001*
Hematoma	10	5.0	1	1.6	0.47	10	5.0	1	1.6	0.47	10	5.0	1	1.6	0.47
Calcification	17	8.4	21	34.4	0.001*	4	2.0	8	13.1	0.001*	16	7.9	21	34.4	0.001*
Edema	202	100.0	23	37.7	0.001	202	100	23	37.7	0.001	202	100	23	37.7	0.001*
Cysts	91	45.0	15	24.6	0.004*	111	55.0	18	29.5	0.001*	139	68.8	29	47.5	0.001*
Single	28	13.9	12	19.7	0.27	40	19.8	13	21.3	0.79	60	29.7	17	27.9	0.78
Multiple	63	31.2	3	4.9	0.001*	71	35.1	5	8.2	0.001*	79	39.1	12	19.7	0.005*
Trabeculation	10	5.0	0	0.0	0.12	20	9.9	0	0	0.005*	40	19.8	2	3.3	0.002*
Thin wall	26	12.9	14	23.0	0.005*	38	18.8	14	23.0	0.48	61	30.2	24	39.3	0.18
Thick wall	65	32.2	1	1.6	0.001*	73	36.1	4	6.6	0.00*	79	39.1	5	8.2	0.001*
Diameter cm															
Median (range)	4.8 (1.5–10)		4 (1.5–7)		0.001*	5.1 (1.7–10.1)		4.5 (1.7–7.1)		0.001*	5.1 (1.9–10.8)		4.7 (1.9–7.8)		0.001*
Hypo	170	84.2	56	91.8	0.13	181	89.6	54	88.5	0.81	80	39.6	6	9.8	0.001*
Hyper	32	15.8	5	8.2		21	10.4	7	11.5		122	60.4	5	90.2	
Homogeneity															
Homogenous	40	19.8	55	90.2	0.001*	10	5.0	51	83.6	0.001*	6	3.0	49	80.3	0.001*
Heterogeneous	162	80.2	6	9.8		192	95.0	5	16.4		196	97.0	12	19.7	

*$P < 0.05$ significant

IOUS (intraoperative ultrasound), CT (computed tomography), MRI (magnetic resonance imaging), HG (high grade), LG (low grade)

- Heterogeneity was found to be significant ($P=0.001$), with metastases at 98%, gliomas at 82%, other tumors at 71%, and meningiomas at 30%.
- A cystic component was significantly found in gliomas (85%), other lesions (38%), metastases (35%), and meningiomas (20%). Cystic criteria were also significant leading factors. Table 6

From previous results, we can suspect meningioma if the lesion was under the dura with a regular contour, calcifications, and a homogenous hyper-echoic component. Metastases were suspected if the lesion was regular in contour, hypo-echoic, heterogeneous, necrotic, surrounded by edema, and devoid of calcification. Gliomas are suspected to be hyper-echoic, heterogeneous, surrounded by edema, have a cystic component, and may have necrosis and/or calcification. Figures 6 and 7

We can represent the ability of intraoperative ultrasound to characterize the gross pathological features of intraventricular tumors in comparison with CT and MRI as lateral ventricular tumors (epidermoid and choroid plexus papillomas) and fourth ventricular tumors (medulloblastoma and ependymoma) are well demarcated for their gross internal and external features by IOUS in Fig. 8

(See figure on next page.)

Fig. 3 Imaging of low-grades glioma (6 different cases) by MRI with contrast, CT with contrast and IOUS**.** All lesions are not enhanced in CT and MRI images. Cases **a**, **b**, **c**: White arrows refer to calcifications (hyper-dense in CT and hyper-echogenic in IOUS). Case **d**: Pilocytic astrocytoma; arrows 1 refer to large cystic part, arrows 2 refer to small fleshy part with best delineation in IOUS images. Cases **e**, **f**: Astrocytoma grade 2; arrows 3 refer to the fleshy lesion which appeared hypo-intense in MRI T1, hypo-dense in CT and hyper-echogenic with best delineation in IOUS. The ultrasound criteria of low-grades tumors as noted in these cases are calcifications **a**, **b**, **c**, regular contours, hyper-echogenicity, homogeneity, single cyst (d), and few amount of brain edema

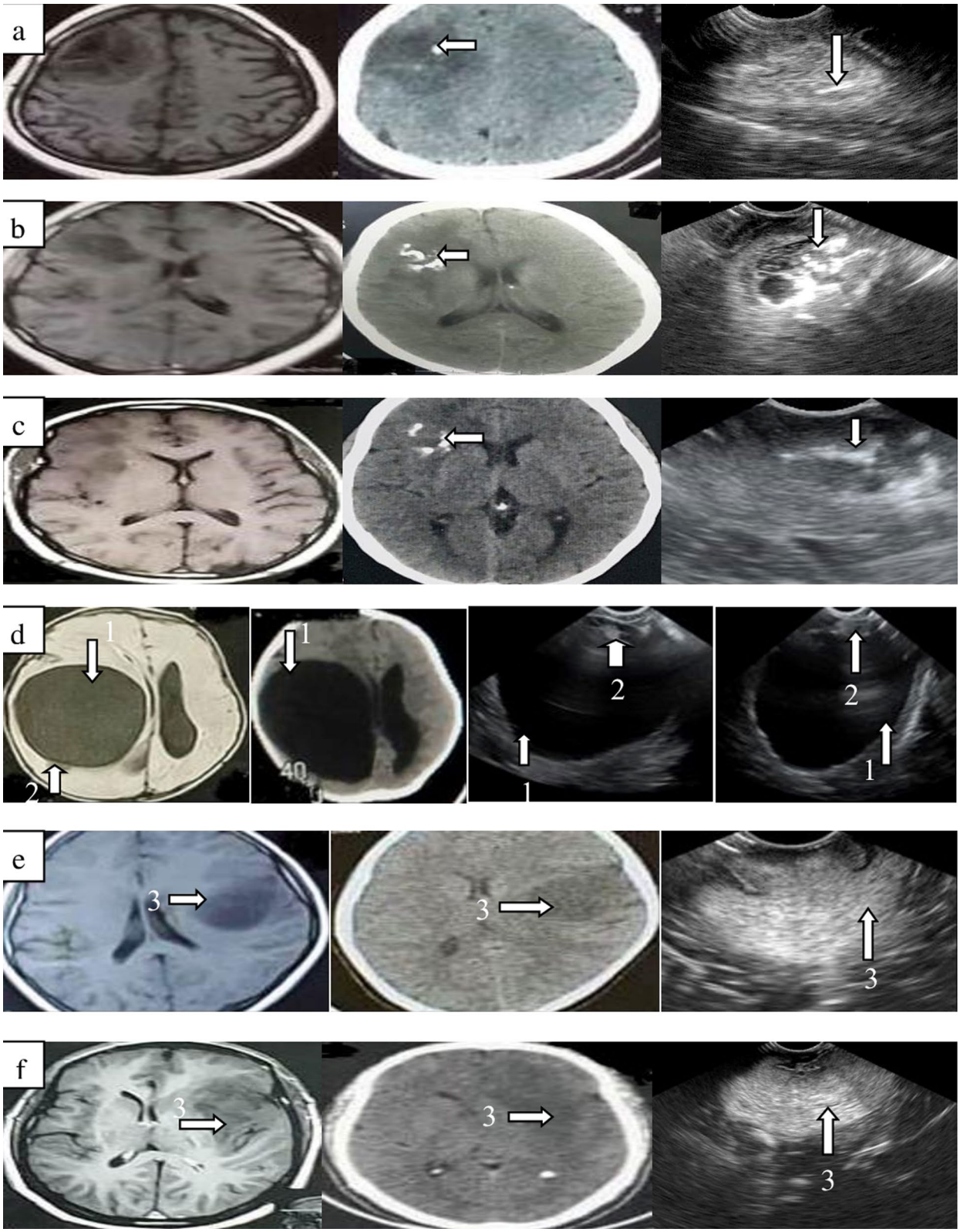

Fig. 3 (See legend on previous page.)

Discussion

The echogenic definitions of the brain mass lesions by intraoperative ultrasound were analyzed and compared to the preoperative imaging and postoperative histopathological data to evaluate reality and characterize different mass lesions pathology by IOUS. In this study, the brain abscess wall appeared hyper-echoic like a ring enhancement with heterogeneous hypo-echoic content and surrounded by hyper-echoic brain edema in all cases. IOUS was significantly superior on CT with contrast in brain abscess wall delineation and equal to MRI T1 with contrast, although no contrast was used with IOUS. Our results were documented in multiple works as Wang et al. [10] described mature abscesses by ultrasound imaging as having heterogeneous hypo-echoic internal contents with a spontaneous contrast-like wall. Chandler and Rubin [4] mentioned that brain abscesses of different dimensions and consistencies were well delineated with IOUS, and the center appears low to high echoic according to the stage of abscess formation. Sosna et al. [11] characterized IOUS imaging of brain abscesses by an obvious hyper-echoic wall and an internal content of variable echogenicity according to its contents of necrosis and debris. Enzmann et al. [12] also described brain abscesses as having iso- to hypo-echogenic content and a hyper-echoic wall by IOUS. Patil et al. [13] described a mature brain abscess as having a regular margin with hypo-echoic contents. Brain abscesses of different sizes and consistency can be well delineated with ultrasound. According to the stage of the abscess, the center may be of different echogenicity [14]. The ultrasound provided more accurate neuropathologic characteristics of the brain abscess than the CT scan [15].

The ultrasound delineated all intra-parenchymal brain hematomas, with characterization of the shape, dimensions, surrounding edema, and age of the blood. The echogenicity varied according to the age of the blood, as acute hematomas up to two days old appeared hyper-echogenic and older hematomas appeared more and more hypo-echogenic. Intra-parenchymal brain hematomas, either acute or sub-acute, are seen as hyper-echogenic mass lesions [14]. Brain hematomas up to a few days old are imaged as hyper-echogenic mass lesions. After a week to ten days, clot breakdown and red cell destruction tend to make the hematoma appear more and more hypo-echoic [4]. Van Velthoven [16]'s study documented different results, as in comparing CT and MRI to IOUS in the evaluation of brain hematomas, he found the borders were not demarcated as in CT and MRI. In other studies, the comparison to preoperative CT brain and MRI showed that IOUS can detect small and large hematomas with great delineation, equivalent to CT and MRI [17–19].

In this study; the brain tumors pathological characters were different according to grading and type. IOUS showed great power of delineation of tumor characters more than CT and MRI T1; IOUS showed significant definition of brain tumors more than CT and MRI T1 regarding tumor edges definition, tumor contours, necrosis, cystic components (cystic definition, cystic multiplicity, cystic trabeculations, and cystic wall thickness), hyper-gray scale, and heterogeneity. IOUS was equivalent to CT regarding calcification, intra-tumoral hematomas, and brain edema. IOUS was significantly better than MRI T1 regarding intra-tumoral calcification and equivalent regarding hematoma and edema. The IOUS measures of tumors were found to be larger than CT and MRI but not statistically significant, which may be due to multi-directional measurement compared to CT and MRI, a delay between imaging dates, different tumor cell infiltration detection, or different tissue representation. Regarding the tumor color (gray scale) in CT, MRI, and sonar, the different mechanisms of working between these machines make the tumor components appear different in gray scales.

(See figure on next page.)

Fig. 4 Imaging of high-grades glioma by MRI with contrast, CT with contrast and IOUS**.** Cases **a**, **b**, **c** astrocytoma grade 3; arrows 1 refer to cystic part and arrows 2 refer to fleshy part with heterogeneous enhancement in MRI, faintly enhanced CT in case **b**, IOUS delineated well the fleshy part (hyper-echogenic) and the cystic parts (hypo-echogenic) and low edema in all images. Cases **d**, **e**, **f**; astrocytoma grade 4. Case **d**; arrows 3 refer to cystic part and arrows 4 refer to fleshy part which more delineated in IOUS image. Case **e**; arrows 3 refer to content of the lesion which appeared cystic in MRI and CT images but fleshy in IOUS image (mixed echogenicity) which matched intraoperative findings. Arrows 4 refer to mass boundaries which delineated well in all images. Case **f**; arrows 3 refer to content of the lesion which appeared fleshy with necrosis in all images but small cysts appeared in IOUS image and arrows 4 refer to mass boundaries which less delineated in CT image. The ultrasound criteria of high-grades tumors as noted in these cases are irregular contours (**a**, **b**), necrosis (**e**, **f**), brain edema(all), presence of cystic component, cystic multiplicity, cystic trabeculations, thick cystic walls (all except e), hypo-echogenicity (**b**, **e**, **f**), and heterogeneity

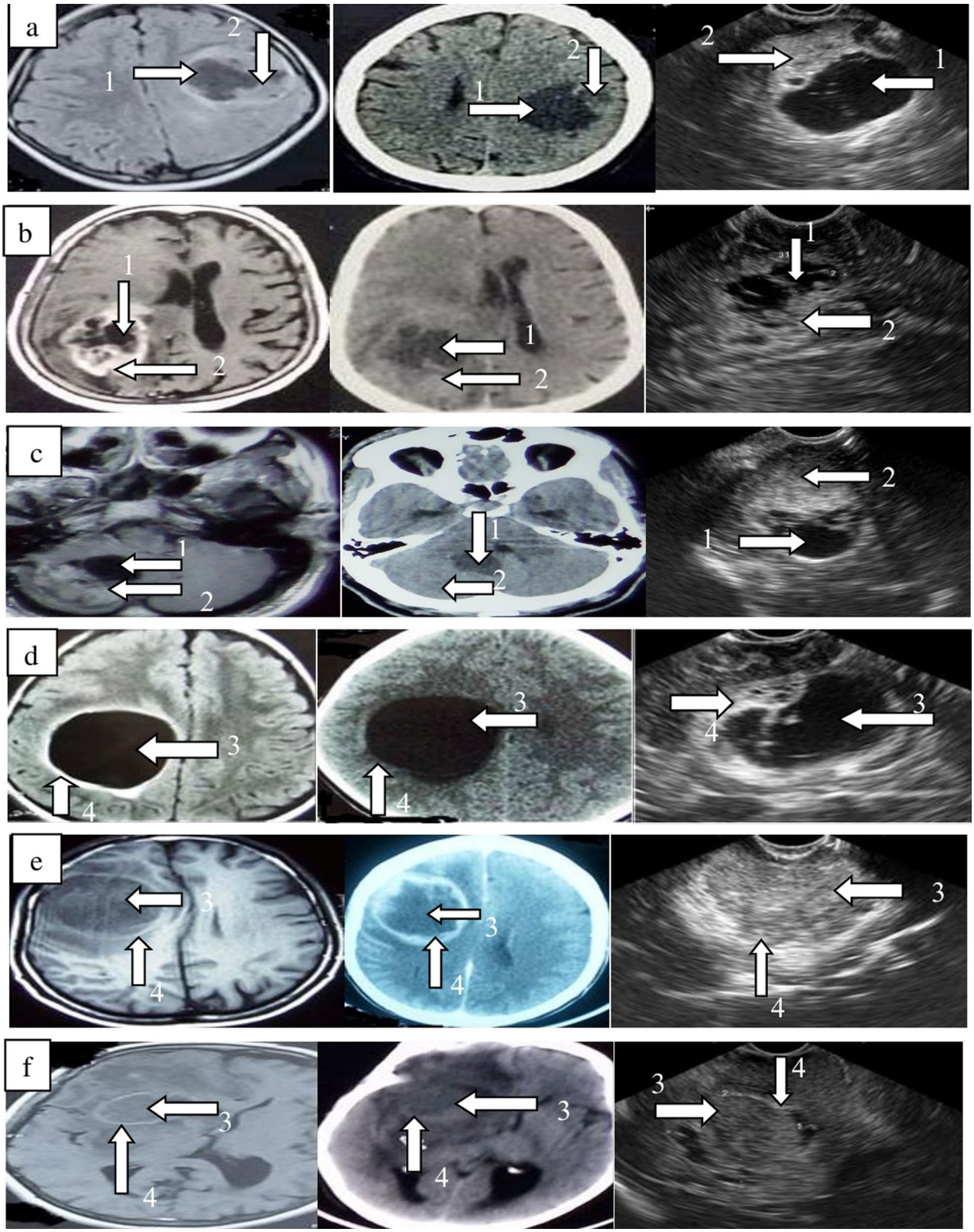

Fig. 4 (See legend on previous page.)

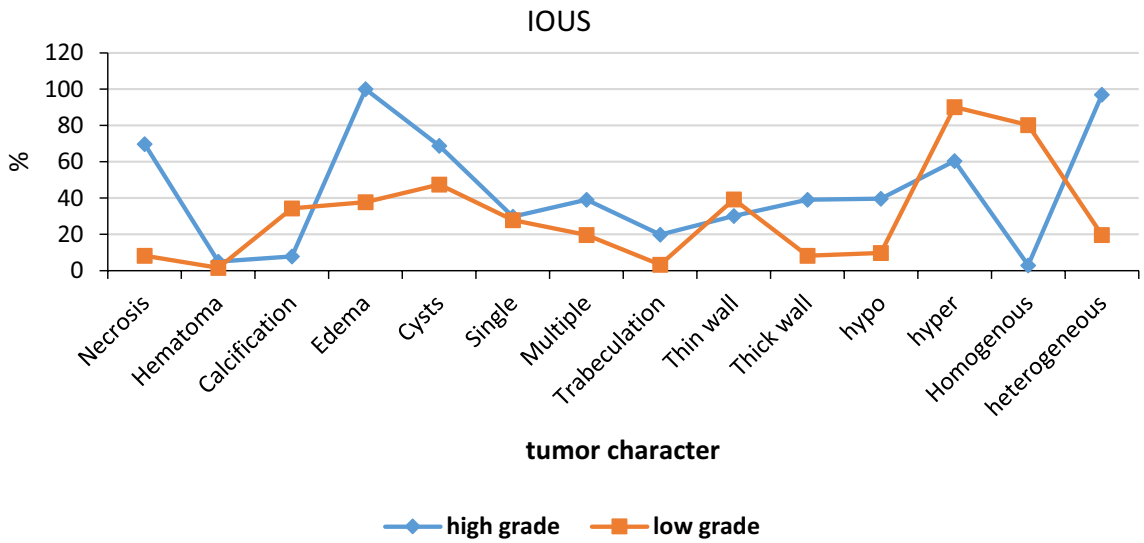

Fig. 5 Graph demonstrating the brain tumors grading; high grade (HG) versus low grade (LG) according to IOUS imaging

Several studies evaluated the capability of IOUS to detect tumor pathology and characteristics. Panagiota and Pallikarakis [5] detailed that IOUS is even better at delineating the cystic, necrotic, and solid parts than CT. Calcification inside brain tumors produces strong echos, while cysts and necrosis produce weak echos. Chen et al. [20] mentioned that IOUS introduces great details of intracranial lesions as well as or even better than CT and MRI brain. Camp et al. [21] found that IOUS can detect necrosis before detection by CT or MRI of the brain. Leroux et al. [22] and Koivukangas et al. [23] confirmed the ability of ultrasound to distinguish between tumor and edema when CT was equivocal and IOUS was more accurate than CT in the definition of brain glioma. Leroux et al. [22] documented the ability of IOUS to detect infiltrating tumor cells better than T1 MRI and differentiate brain edema as T2 imaging from tumor and normal brain. Chandler and Rubin [4] stated that IOUS can define low-grade gliomas much better than CT, and in cystic brain lesions, IOUS can detect the solid part that does not appear on CT. In high-grade gliomas, the IOUS is better than CT at differentiating cystic parts from necrosis. Low-grade tumors were more echogenic, with well-defined borders. Reinacher and Van Velthoven [24] and Auer and Van Velthoven [17] documented that IOUS can delineate internal characteristics of brain mass lesions better than CT and MRI but is equivocal or less accurate in delineating the border, which is in contrast to our findings. Unsgaard et al. [25] experienced that IOUS were comparable to or even better than MRI regarding landmarks of brain tumors. Moiyadi and Shetty. [26] stated that numerous studies approved better demarcation of brain metastases, malignant tumors, and benign tumors by IOUS than CT and that it was powerful in differentiating solid and cystic lesions. Tumor sizes were different between sonar and MRI. LeRoux et al. [22] demonstrated sonar overestimation but not statistical significance, as our results also [7, 24], and [27] documented this observation. Gooding et al. [28] noted that high-density masses by CT are always solid on IOUS, while low-density masses by CT may be either cystic or solid on IOUS, so IOUS is more accurate in cystic lesions definition. Also, Kane [29] stated that many brain lesions that were cystic on CT were solid on IOUS, and cystic brain tumors were extremely well characterized by IOUS, with various trabeculations and solid parts helping complete tumor resection. Koivukangas [30] found a difference between CT density and sonar echogenicity without any relation. Ferrigno and Foroni [31] reported that MRI T1 and sonar images are equivalent in terms of gray scale, as both can show soft tissues well, delineate the periphery in high gray, and show cystic and necrotic parts in low gray scales, so both are similar and comparable.

The grading criteria of brain tumors (high versus low grades) can be evaluated by IOUS with significant correlation to the WHO grading system. Tumors of large sizes increase the diagnosis toward high grading. The criteria for high grading increase with the irregularity of the edges and the heterogeneity of the tumor. Low-grades tumors showing a high echogenicity with a better border delineation [32]. Rogers et al. [33] described benign tumors according to the well-margin definition by IOUS.

Table 6 IOUS criteria of tumors types

	Glioma high grade n.125		Glioma low grade n.33		Total glioma n.158		Metastasis n.43		Meningioma n.20		Other n.42		*P*
	n	%	*n*	%	*n*	%	*n*	%	*n*	%	*n*	%	
Well-defined edge	108	86.4	31	93.9	139	88.0	40	93.0	20	100.0	41	97.6	0.09
	P = 0.24												
Regular contour	48	38.4	20	60.6	68	43.0	32	74.4	18	90.0	37	88.1	0.001*
	P = 0.021*												
Necrosis	90	72.0	1	3.0	91	57.6	33	76.7	4	20.0	18	42.9	0.001*
	P = 0.001*												
Hematoma	4	3.2	0	0.0	4	2.5	3	7.0	0	0.0	4	9.5	0.12
	P = 0.77												
Calcification	13	10.4	12	36.4	25	15.2	0	0	9	45.0	5	11.9	0.004*
	P = 0.001*												
Edema	125	100.0	24	72.7	149	94.3	43	100	10	50.0	35	83.3	0.001*
	P = 0.001*												
Cysts	113	90.4	21	63.6	134	84.8	15	34.9	4	20.0	16	38.1	0.001*
	P = 0.001*												
Single	50	40.0	13	39.4	63	39.9	7	16.3	2	10.0	6	14.3	0.001*
	P = 0.95												
Multiple	63	50.4	8	24.2	71	44.9	8	18.6	2	10.0	10	23.8	0.001*
	P = 0.007*												
Trabeculation	38	30.4	2	6.1	40	24.7	3	7.0	0	0	0	0	0.001*
	P = 0.004*												
Thin wall	41	32.8	19	57.6	60	38.0	10	23.3	3	15.0	12	28.6	0.07
	P = 0.009*												
Thick wall	71	56.8	2	6.1	73	46.2	5	11.6	1	5.0	3	7.1	0.001*
	P = 0.001*												
Main echogenicity													
Hyper-echogenic	75	60.0	30	90.9	105	66.5	19	44.2	20	100.0	32	76.2	0.001*
	P = 0.001*												
Heterogeneous	123	98.4	7	21.2	130	81.6	42	97.7	6	30.0	30	71.4	0.001*
	P = 0.001*												
Total	125	100.0	33	100.0	158	100.0	43	100.0	20	100.0	42	100.0	

*$P < 0.05$ significant

IOUS (intraoperative ultrasound)

Chacko et al. [34] found that all tumors were hyperechoic on IOUS irrespective of pathology, which was not matched with our results.

Brain tumors types can be specified by IOUS in certain situations, as gross pathology specification of tumors types is not supported by any imaging and requires extensive histopathological examinations. Patil et al. [13] described meningiomas on IOUS as having 100% well-delineated borders, 95% homogenous mass, 93% hyperechogenicity, and being surrounded by brain edema in 449% of cases. Ang et al. [35] described meningiomas in IOUS as hyper-echogenic. Meningiomas are the most hyper-echogenic brain mass lesion, especially if calcifications are present [5]. Chen et al. [18] demonstrated pathological characteristics of brain mass lesion by IOUS: meningiomas were mostly heterogeneous and hyperechogenic masses; low-grade gliomas were iso-echogenic or hyper-echogenic masses; high-grade gliomas and metastases were hypo-echogenic to hyper-echogenic masses. Van Velthoven [16]'s work on 374 cases of IOUS

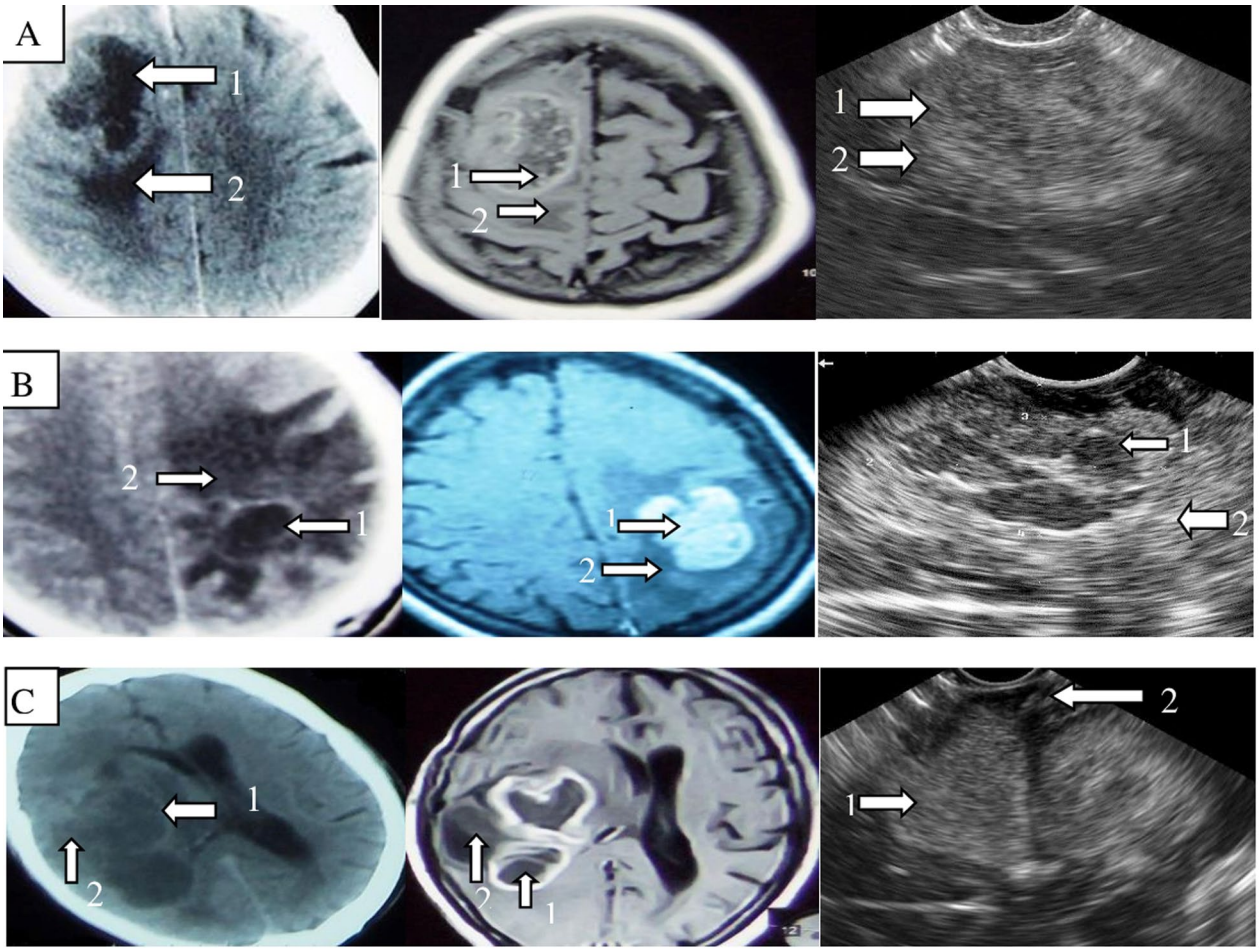

Fig. 6 Imaging of brain metastases by CT with contrast, MRI with contrast and IOUS. Arrows 1 refer to the fleshy tumor and arrows 2 refer to brain edema. Case **a**: Well-defined fleshy mass with heterogeneous enhancement and central necrosis in CT and MRI. Well-defined fleshy mass with hyper-echogenic periphery and hypo-echogenic center in IOUS. Case **b**: Ill-defined mass with heterogeneous enhancement in CT and well defined with homogenous enhancement in MRI. Well-defined fleshy mass mostly hypo-echogenic in IOUS. Case **c**: Ill-defined mass with heterogeneous enhancement in CT and well defined with heterogeneous enhancement in MRI. Well-defined fleshy mass with heterogeneous hyper-echogenicity in IOUS. The ultrasound criteria of high-grades tumors as noted in these cases are irregular contours, necrosis, brain edema, hypo-echogenicity, and heterogeneity

brain metastases detailed that IOUS brain metastases were mostly homogenous, had different echogenicity with a hyper-echoic border, and were well delineated in most cases. The meningioma was well defined, hyper-echogenic, and homogenous. Picarelli et al. [36]'s work on brain metastases found IOUS criteria of well-defined borders, hyper-echogenicity, and homogenous masses in all solid tumors except breast intra-ductal carcinomas, which were solid but hypo-echogenic. Necrosis, cysts, and hemorrhage were hypo-echogenic. Wang et al. [37] found that most high-grade gliomas were heterogeneous, hypo-echogenic, irregular contour, indistinct margin, tumor necrosis, and surrounded by brain edema by IOUS. Shi et al. [38] detailed the ultrasound differences between low grades and high grades, which match our findings. Unsgaard et al. [7] found IOUS agreement with histopathology in 73% of benign gliomas, 83% of anaplastic gliomas, 80% of glioblastoma multiforms, and 100% of metastases, which were better than MRI, especially with low-grade gliomas.

Other brain tumors, like intraventricular tumors, were well managed by IOUS in this study due to the ability to

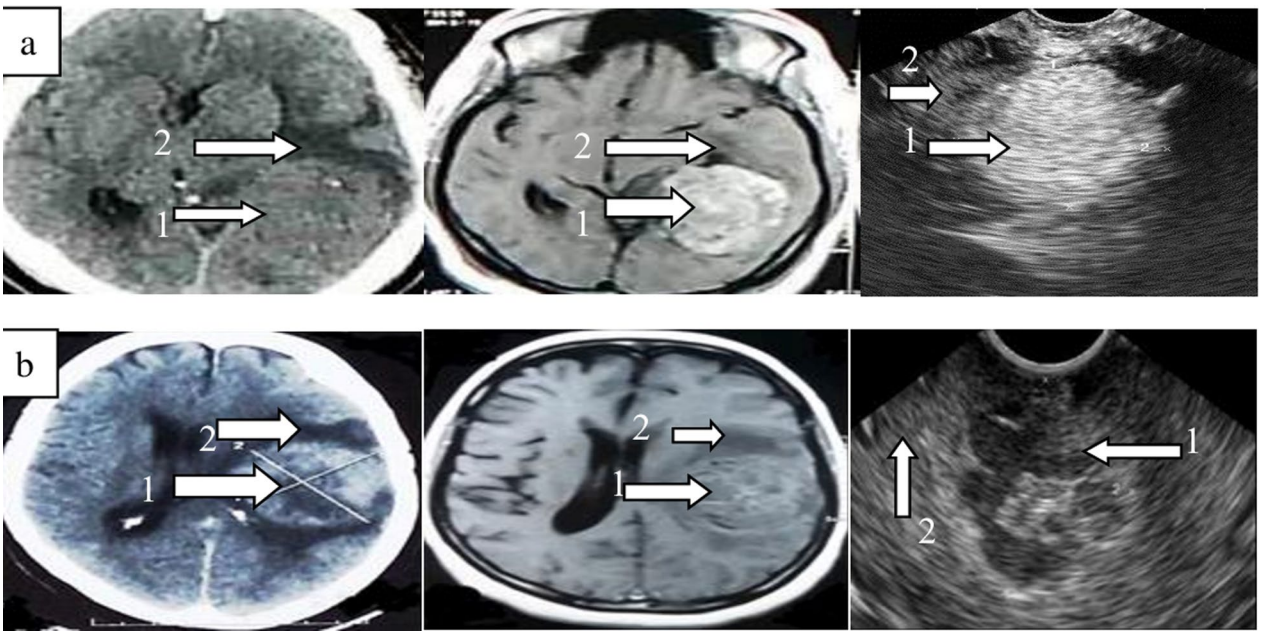

Fig. 7 Imaging of meningioma by CT with contrast, MRI with contrast and IOUS. Arrows 1 refer to the fleshy tumor and arrows 2 refer to brain edema. Case **a**: Ill-defined mass without enhancement in CT and well defined with homogenous enhancement in MRI. Well-defined fleshy mass with homogenous hyper-echogenicity in IOUS. Case **b**: Well-defined fleshy mass with heterogeneous enhancement and necrosis in CT and MRI. Well-defined fleshy mass with hyper-echogenic periphery and hypo-echogenic center in IOUS**.** The ultrasound criteria of low-grades tumors as noted in case **a** are regular contours, hyper-echogenicity, homogeneity, and few amount of brain edema. The ultrasound criteria of high-grades tumors as noted in case **b** are irregular contours, necrosis, brain edema, hypo-echogenicity, and heterogeneity

identify the pathological origin of the tumor as from the roof or the floor of the fourth ventricle, or the choroid plexus, in addition to the definition of external and internal features. Nagaty et al. [39] found that IOUS during posterior fossa tumor resection was of excellent value in resection and definition of the tumor borders and contents of solid and cystic parts.

This study provided a collection of different brain pathologies imaged by conventional ultrasound to encourage the use of this valuable aid during brain surgeries. Beside pathological definition, the IOUS can also define brain anatomical landmarks and assist in safe gross total resection; these were documented recently by Dixon et al. [40] and Frassanito et al. [41] with recommendation to make IOUS as a routine neurosurgical tool and encourage the training by spending some time performing pre-IOUS to scan the surgical field on planes comparable to preoperative MRI to maintain a correct orientation of the anatomical and pathological situation.

Multiple advances of intraoperative ultrasounds in recent years as 3D, contrast enhancing, and navigator coupling provided more surgical orientation and this field still of need for more innovations [42].

Conclusion

The intraoperative ultrasound during brain surgeries has a role in defining the internal and external gross pathological features of all non-traumatic mass lesions. The walls of the brain abscesses were significantly well defined in IOUS imaging in comparison with CT and equivalent to MRI. IOUS showed equivalent significance to CT and MRI in characterizing intra-parenchymal brain hematomas. IOUS showed significant definition of brain tumors in comparison with CT and MRI regarding tumor edges, contours, necrosis, and cystic components. The significant criteria for high-grade brain tumors by IOUS were the presence of necrosis, brain edema, cystic components with thick walls and trabeculations, large diameter, hypoechogenicity, heterogeneity, and irregular contour.

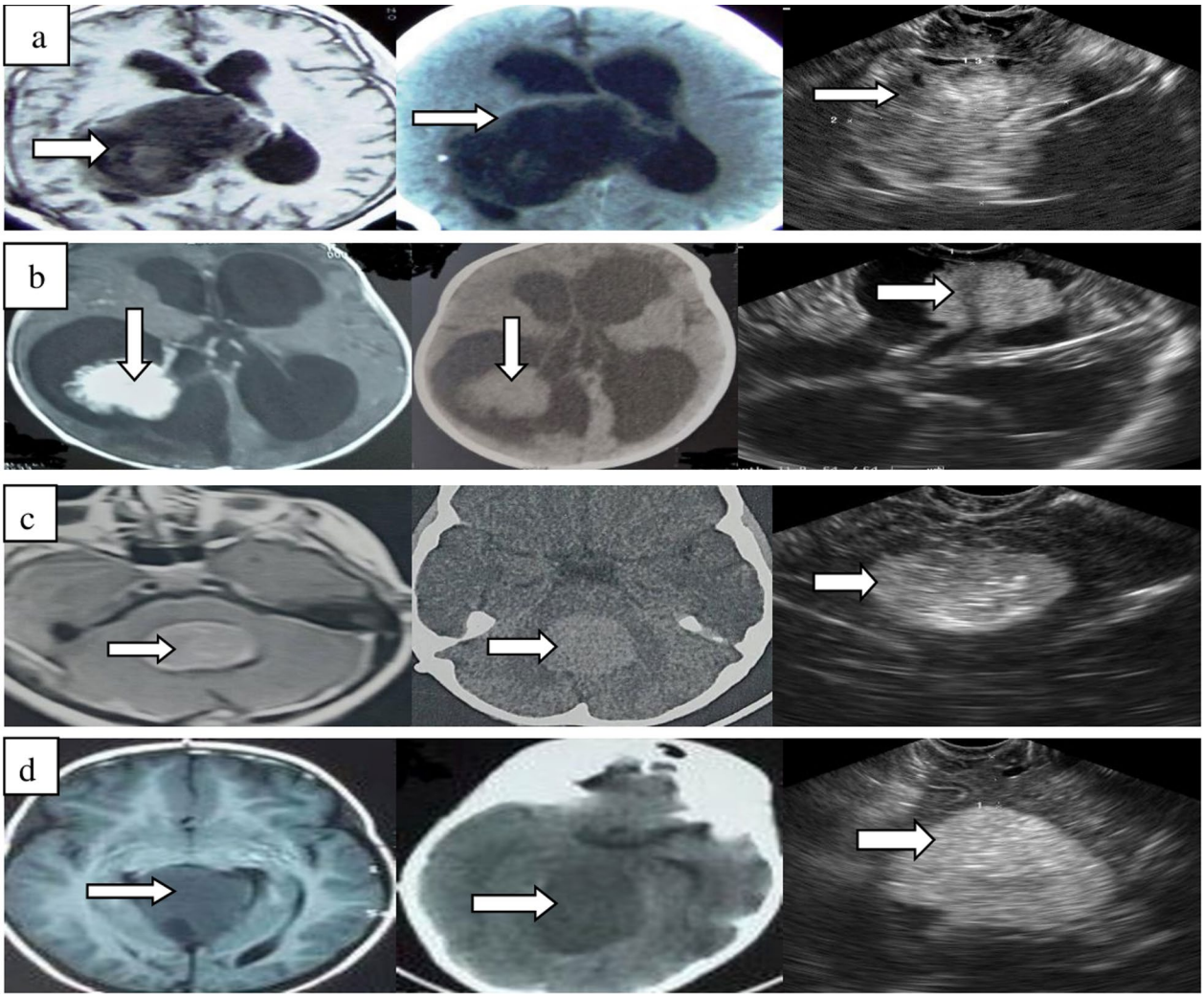

Fig. 8 Imaging of intraventricular tumors by MRI T1, CT and IOUS. White arrows refer to the tumor. Case **a**: Intraventricular epidermoid tumor; hypo-intense in MRI T1, hypo-dense in CT, and heterogeneous echogenicity in IOUS. Case **b**: Intraventricular choroid plexus papilloma; homogenous enhancement in MRI T1, hypo-dense in CT and homogenous hyper-echogenicity in IOUS. Case **c**: Intraventricular ependymoma; heterogeneous enhancement in MRI T1, hyper-dense in CT and heterogeneous echogenicity in IOUS. Case **d**: Intraventricular medulloblastoma; hypo-intense in MRI T1, hypo-dense in CT, and homogenous hyper-echogenic in IOUS

Abbreviations

CT	Computed tomography
MRI	Magnetic resonance imaging
IOUS	Intraoperative ultrasound
MHZ	Megahertz
HG	High grade
LG	Low grade
WHO	World Health Organization

Acknowledgements
It is lucky to work with the neurosurgery team at Zagazig university hospital for great help and support.

Author contributions
The author contributed to the study conception, design, most surgical works, data collection, and drafting the manuscript. The author read and approved the final manuscript.

Funding
All patients operated at Zagazig university hospitals neurosurgery department for free.

Availability of data and materials
All data that support the findings of this study are available from the neurosurgery department Zagazig university hospital. Data are, however, available from the author when requested with permission.

Declarations

Ethics approval and consent to participate
A research committee approval has been granted for this study by the medical ethics committee, ZU-IRB#9654-24-7-2022. Informed consent according to the criteria set by the local research ethics committee in our center obtained in writing before surgery. If consent could not be obtained because the patient

was in disturbed consciousness or young age (< 18 years), it was obtained from relatives.

Consent for publication
Informed consents were obtained for all patients and no personal data included in this study.

Competing interests
The author declares that they have no competing interests.

Received: 23 March 2023 Accepted: 22 July 2023
Published online: 16 April 2024

References

1. Tumturk AF, Kucuk A, Ulutabanca H, Menku A, Gergin S, Oral S. The impact of the use of neuronavigation together with intraoperative ultrasonography in minimally invasive intracranial cavernous hemangioma surgery. Erciyes Med J. 2014;36(4):161–5.
2. Del Bene M, DiMeco F, Unsgård G. Intraoperative ultrasound in brain tumor surgery: state-of-the-art and future perspectives. Front Oncol. 2021;11:780517. https://doi.org/10.3389/fonc.2021.780517.
3. Homapour B, Bowen JE, Want EJ, O'Neil K, Apostolopoulos V, Nandi D, Van Dellen JR, Roncaroli F. Intraoperative real time three-dimensional ultrasound assisted positioning of catheters in the microdialysis of glial tumors. J Clin Neurosci. 2010;4:506–10.
4. Chandler WF, Rubin IM. The application of ultrasound during brain surgery. World J Surg. 1987;11:558–69.
5. Unsgaard G, Selbekk T, Brostrup MT, Ommedal S, Torp SH, Myhr G, Bang J, Nagelhus Hernes TA. Ability of navigated 3D ultrasound to delineate gliomas and metastases-comparison of image interpretations with histopathology. Acta Neurochir (Wien). 2005;147:1259–69.
6. Panagiota K, Pallikarakis N. Simulation of ultrasound brain cancer imaging. Master's Thesis University of Patras, Faculty of Medicine 2011; 1–108
7. Hartov A, Roberts DW, Paulsen KD. A comparative analysis of coregistered ultrasound and magnetic resonance imaging in neurosurgery. Oper Neurosurg. 2008;62:95–101.
8. Mair R, Heald J, Poeata I, Ivanov M. A practical grading system of ultrasonographic visibility for intracerebral lesions. Acta Neurochir (Wien). 2013;155(12):2293–8. https://doi.org/10.1007/s00701-013-1868-9.
9. Louis DN, Perry A, Reifenberger G, von Deimling A, Figarella-Branger D, Cavenee WK, Ohgaki H, Wiestler OD, Kleihues P, Ellison DW. The 2016 World Health Organization classification of tumors of the central nervous system: a summary. Acta Neuropathol. 2016;131(6):803–20. https://doi.org/10.1007/s00401-016-1545-1.
10. Wang J, Duan YY, Liu X, Wang Y, Gao GD, Qin HZ, Wang L. Application of intraoperative ultrasonography for guiding microneurosurgical resection of small subcortical lesions. Korean J Radiol. 2011;12(5):541–6.
11. Sosana J, Barth MM, Kruskal JB, Kane RA. Intraoperative sonography for neurosurgery. J Ultrasound Med. 2005;24:1671–82.
12. Enzmann DR, Lyons BE, Caroll B, Placonee RC, Rasor J, Britt RH, Buxton J, Wilson D. Experimental brain abscess enhanced sonography and pathological correlation. Am J Neuroradiol. 1982;3:41–5.
13. Patil D, Sharma V, Tiwari VDP. Intraoperative ultrasound in intracranial space occupying lesions. World J Surg Med Radiat Oncol. 2013;7:5–9.
14. Velho V, Kharosekar HU, Bhople L, Domkundwar S. Intraoperative ultrasound an economical tool for neurosurgeons: a single-center experience. Asian J Neurosurg. 2020;15(4):983–8. https://doi.org/10.4103/ajns.AJNS_332_20.
15. Enzmann DR, Britt RH, Carroll BLB, Wilson DA, Buxton J. High-resolution ultrasound evaluation of experimental brain abscess evolution: comparison with computed tomography and neuropathology. Radiology. 1982;142:95–102.
16. Van Velthoven V. Intraoperative ultrasound imaging: comparison of pathomorphological findings in US versus CT MRI and intraoperative findings. Acta Neurochir (Suppl). 2002;85:95–9.
17. Auer LM, Van Velthoven V. Intraoperative ultrasound imaging: comparison of pathomorphological finding in US and CT. Acta Neurochir (Wien). 1990;104:84–95.
18. Chen SY, Chiou TL, Chiu WT, Su CF, Lin SZ, Wang SG, Yen PS. Application of intraoperatiev ultrasound for brain surgery. Tzu Chi Med J. 2004;16(2):85–92.
19. Park J, Woo H, Kim GCH. Diagnostic usefulness of intraoperative ultrasound for unexpected severe brain swelling in ultra-early surgery for rupture intracranial aneurysm. Acta Neurochir. 2012;154:1869–75.
20. Chen SS, Shao KN, Chiang JH, Chang CY, Lao CB, Lirng JF, Teng MM. Intracranial pathology: Comparison of intraoperative ultrasonography with computed tomography, and magnetic resonance imaging. Zhonghua Yi Xue Za Zhi (Taipei). 1999;62(8):521–8.
21. Camp S, Apostolopoulos V, Raptopoulos V, Nandi D. Objective image analysis of real-time three-dimensional intraoperative ultrasound for intrinsic brain tumor surgery. J Ther Ultrasound. 2017;5:2.
22. Leroux PD, Winter TC, Berger MS, Mack LA, Wang K, Elliott JP. A comparison between preoperative magnetic resonance and intraoperative ultrasound tumor volumes and margins. J Clin Ultrasound. 1994;22:29–63.
23. Koivukangas J, Louhisalmi Y, Alakuijala J, Oikarinen J. Ultrasound controlled neuronavigator guided brain surgery. J Neurosurg. 1993;79:36–42.
24. Reinacher PC, Van Velthoven V. Intraoperative ultrasound imaging: practical applicability as a real time navigation system. Acta Neurochir. 2003;85:89–93.
25. Unsgaard G, Gronningsaeter A, Ommedal S, Nagelhus Hernes TA. Brain operations guided by two-dimensional ultrasound: New possibilities as a result of improved image quality. Neurosurgery. 2002;51:402–12.
26. Moiyadi A, Shetty P. Objective assessment of utility of intraoperative ultrasound in resection of central nervous system tumors: a cost-effective tool for intraoperative navigation in neurosurgery. J Neurosci Rural Pract. 2011;2:4–11.
27. Lindseth F, Kaspersen JH, Ommedal S, Hernes TAN. Multimodal image fusion in ultrasound-based neuronavigation: improving overview and interpretation by integrating preoperative MRI with intraoperative 3D ultrasound. Comput Aid Surg. 2003;8:49–69.
28. Gooding GAW, Boggan JE, Weinstein PR. Characterization of intracranial neoplasms by CT and intraoperative sonography. AJNR. 1984;5:517–20.
29. Kane RA. Intraoperative ultrasonography. J Ultrasound Med. 2004;23:1407–20.
30. Koivukangas J. Ultrasound imaging in operative neurosurgery. Acta Univ. 1984;115:35–150.
31. Ferrigno G, Foroni R. Stand-alone intraoperative ultrasound imaging for neurosurgery. Corso di laurea magistral in ingeneria biomedical, politecnico Di Melano. 3013: 29–25.
32. Giammalva GR, Ferini G, Musso S, Salvaggio G, Pino MA, Gerardi RM, Brunasso L, Costanzo R, Paolini F, Di Bonaventura R, Umana GE, Graziano F, Palmisciano P, Scalia G, Tumbiolo S, Midiri M, Iacopino DG, Maugeri R. Intraoperative ultrasound: emerging technology and novel applications in brain tumor surgery. Front Oncol. 2022;12:818446. https://doi.org/10.3389/fonc.2022.818446.
33. Rogers JV, Shuman WP, Hirsch JH, Lang S, Howe J, Burchiel K. Intraoperative neurosonography: application and technique. Am J Neuroradiol. 1984;5:755–60.
34. Chacko AG, Kumar NK, Chacko G, Athyal R, Rajshekhar V. Intraoperative ultrasound in determining the extent of resection of parenchymal brain tumors. A comparative study with computed tomography and histopathology. Acta Neurochir. 2003;145:743–8.
35. Tang H, Sun H, Xie L, Tang Q, Gong Y, Mao Y, Xie Q, Zheng M, Wang D, Zhu H, Zhu J, Feng X, Yao Z, Chen X, Zhou L. Intraoperative ultrasound assistance in resection of intracranial meningiomas. Chin J Cancer Res. 2013;25(3):339–45.
36. Picarelli H, Oliveira ML, Bor-Seng-Shu E, Ribas ESC, Santos AM, Teixeira MJ. Intraoperative ultrasonography for presumed brain metastasis: a case series study. Arq Neuro-psiquiatr. 2012;70(10):793–8.
37. Wang J, Liu X, Hou WH, Dong G, Wei Z, Zhou H, Duan YY. The relationship between intraoperative ultrasonography and pathological grade in cerebral glioma. J Int Med Res. 2008;36:1426–34.

38. Shi J, Zhang Y, Yao B, Sun P, Hao Y, Piao H, Zhao X. Application of multiparametric intraoperative ultrasound in glioma surgery. Biomed Res Int. 2021;2021(16):6651726.
39. Nagaty A, Elsabaa A, Anwer H. Efficacy of intraoperative ultrasound in resection of posterior fossa lesions. Int J Neurosurg. 2019;3(2):13–20. https://doi.org/10.11648/j.ijn.20190302.11.
40. Dixon L, Lim A, Grech-Sollars M, Nandi D, Camp S. Intraoperative ultrasound in brain tumor surgery: a review and implementation guide. Neurosurg Rev. 2022;45(4):2503–15.
41. Frassanito P, Stifano V, Bianchi F, Tamburrini G, Massimi L. Enhancing the reliability of intraoperative ultrasound in pediatric space-occupying brain lesions. Diagnostics. 2023;13(5):971. https://doi.org/10.3390/diagnostics13050971.
42. Šteňo A, Buvala J, Babková V, Kiss A, Toma D, Lysak A. Current limitations of intraoperative ultrasound in brain tumor surgery. Front Oncol. 2021;22(11):659048. https://doi.org/10.3389/fonc.2021.659048.PMID:33828994;PMCID:PMC8019922.

Publisher's Note